Biochemistry **1984**, *23*, 2199–2203

Lowry, O. H., Rosebrough, N. J., Farr, A. L., & Randall, R. J. (1951) *J. Biol. Chem. 193*, 265.

Moore, S., & Stein, W. H. (1963) *Methods Enzymol. 6*, 819.

Parés, X., & Vallee, B. L. (1981) *Biochem. Biophys. Res. Commun. 98*, 122.

Pietruszko, R. (1979) in *Biochemistry and Pharmacology of Ethanol* (Majchrowicz, E., & Noble, E. P., Eds.) Vol. I, pp 87–105, Plenum Press, New York.

Pietruszko, R., Clark, A., Graves, J. M. H., & Ringold, H. J. (1966) *Biochem. Biophys. Res. Commun. 23*, 526.

Ruegg, U. T., & Radinger, J. (1974) *Int. J. Pept. Protein Res. 6*, 447.

Smith, M., Hopkinson, D. A., & Harris, H. (1973) *Ann. Hum. Genet. 37*, 49.

Strydom, D. J., & Vallee, B. L. (1982) *Anal. Biochem. 123*, 422.

Thiers, R. E. (1957) *Methods Biochem. Anal. 5*, 273.

Vallee, B. L., & Bazzone, T. J. (1983) *Isozymes: Curr. Top. Biol. Med. Res. 8*, 219–244.

Von Wartburg, J.-P., Bethune, J. L., & Vallee, B. L. (1964) *Biochemistry 3*, 1775.

Wagner, F., Berger, A. R., & Vallee, B. L. (1983) *Biochemistry 22*, 1857.

Yphantis, D. A. (1964) *Biochemistry 3*, 297.

Bound-Cation Exchange Affects the Lag Phase in Actin Polymerization†

Lewis C. Gershman, Jay Newman, Lynn A. Selden, and James E. Estes*

ABSTRACT: The delay or lag phase at the onset of polymerization of actin by neutral salt is generally attributed to an actin nucleation reaction. However, when nucleation is circumvented by the use of phalloidin-stabilized nuclei, a lag phase persists when Ca^{2+}-containing actin is polymerized with $MgCl_2$. Pretreatment of actin with ethylene glycol bis(β-aminoethyl ether)-*N,N,N',N'*-tetraacetic acid (EGTA) and/or Mg^{2+} shortens or eliminates this lag phase, suggesting that exchange of the actin-bound divalent cation occurs during this nucleation-independent lag phase. Measurement of the actin-bound cation initially and after brief incubation with EGTA/Mg^{2+} directly verifies that Mg^{2+} has replaced Ca^{2+} as the actin-bound cation, producing a highly polymerizable Mg^{2+}-actin species. Bound-cation exchange prolongs the lag phase in actin polymerization and probably explains what has been termed the monomer activation step in actin polymerization.

The early time course in the polymerization of monomeric actin, initiated by the addition of neutral salt, is usually characterized by a delay. This lag phase was first attributed to an actin nucleation step by Oosawa and his colleagues (Kasai et al., 1962; Oosawa & Asakura, 1975), and it is now generally considered that the nucleation process is mainly responsible for the lag phase during the spontaneous polymerization of actin. Recently, a number of investigations (Tobacman & Korn, 1983; Pollard et al., 1982; Cooper et al., 1983; Gilbert & Frieden, 1983; Gershman et al., 1983; Brenner et al., 1983) have suggested that monomer activation and/or exchange of the tightly bound cation on monomeric actin may also be part of the lag phase, particularly when actin containing bound Ca^{2+} is polymerized with $MgCl_2$ (a frequently employed condition for in vitro polymerization studies). However, there has been no direct experimental demonstration of the effect of cation exchange in monomeric actin on the kinetics of polymerization. Such experiments are difficult because of interference from the simultaneously occurring nucleation step. In experiments reported here, the nucleation step was circumvented by adding phalloidin-stabilized nuclei ("seeds") to initiate the polymerization of fluorescent-labeled actin, and the fluorescence intensity was monitored as a measure of polymer formation. Interestingly, when low concentrations of $MgCl_2$ are added to G-actin containing Ca^{2+} as the bound cation, a lag phase still occurs before polymer formation even when seeds are added with $MgCl_2$. If polymerization is initiated with EGTA also present to facilitate removal of the actin-bound Ca^{2+} or if actin is preincubated with a low concentration of $MgCl_2$ before seeds are added, the lag phase is shortened considerably or eliminated. Measurements of the bound-cation content of actin prior to Mg^{2+} addition and again after incubation with EGTA/Mg^{2+} indicate that Mg^{2+} has replaced Ca^{2+} as the bound cation within a time interval comparable to the duration of the nucleation-independent lag phase.

Experimental Procedures

All reagents were analytical grade with ATP and EGTA being purchased from Sigma Chemical Co., phalloidin from Boehringer-Mannheim, ^{45}Ca from New England Nuclear, and N-P[1] from Molecular Probes. All solutions were prepared with doubly distilled water.

Actin was extracted from rabbit acetone powder (Szent-Gyorgyi, 1951) and purified by previously published procedures (Estes et al., 1981), except a Sephacryl S-300 column was used for the column purification step. To label actin with N-P, column-purified actin (ca. 20 μM) was reacted with equimolar N-P dissolved in dimethylformamide (0.1% final concentration) at room temperature overnight in the presence

---

† From the Research Service, Veterans Administration Medical Center, Albany, New York 12208 (L.C.G., L.A.S., and J.E.E.), the Department of Physiology, Albany Medical College, Albany, New York 12208 (L.C.G. and J.E.E.), and the Department of Physics, Union College, Schenectady, New York 12308 (J.N.). *Received October 10, 1983.* This investigation was supported by the Veterans Administration. A preliminary report of this work has been reported (Gershman et al., 1983).

[1] Abbreviations: N-P, *N*-(1-pyrenyl)iodoacetamide; EGTA, ethylene glycol bis(β-aminoethyl ether)-*N,N,N',N'*-tetraacetic acid.

0006-2960/84/0423-2199$01.50/0

of 100 mM KCl, 2 mM $MgCl_2$, 0.02 mM $CaCl_2$, 0.2 mM ATP, 2 mM tris(hydroxymethyl)aminomethane (Tris), pH 7.8, and 0.01% NaN_3 (Kouyama & Mihashi, 1981). With some preparations, the actin was labeled with N-P under the conditions listed but during the course of the initial actin preparation at the 0.1 M KCl wash step following the 0.8 M KCl incubation (Estes et al., 1981) and prior to column purification. No difference was detected in the properties of the actin labeled at either step. It should also be noted that the N-P labeling step is the last step in the preparation of N-P actin that the actin is in contact with $MgCl_2$. The labeled F-actin was then collected by centrifugation at 170000*g* for 2 h and homogenized with and dialyzed against 0.2 mM ATP, 0.02 mM $CaCl_2$, 2 mM Tris, pH 7.8, and 0.01% NaN_3 (dialysis solution) for three or four 12-h periods. Following dialysis, the actin was sonicated for two 10-s intervals before being centrifuged for 3 h at 170000*g*. The labeled actin was further purified by passage through a Sephacryl S-300 column and used within 36 h. Before use, the N-P actin was sometimes diluted with column-purified unlabeled actin until it had a concentration of 5–100% of the total protein present. The fraction of N-P actin in the final solution did not affect the experimental properties of the various actin preparations reported here.

A stock solution of phalloidin-stabilized seeds was prepared by polymerizing unlabeled column-purified actin at a concentration of 25 μM in the absence of salt by incubation for 25 h at room temperature with equimolar phalloidin (Estes et al., 1981). This solution could be stored at 4 °C for periods of over 1 month. To use the seeds, aliquots of the stock solution were diluted 1:10 with dialysis solution and sonicated for two 30-s periods. Electron microscopic examination of such a seed solution showed a field containing an undetermined number of relatively short polymers. These would reanneal upon aging but could be reverted to the seed state by sonication. Since reannealing predominantly occurred immediately following sonication, every seed solution was sonicated and stored on ice at least 3 h prior to an experiment to ensure that the occurrence of the reannealing process during the experiment was negligible. Protein was measured by the method of Bradford (1976) or by ultraviolet absorption (Estes et al., 1981) after correcting for the absorption of N-P at 290 nm ($=0.33A_{344\text{nm}}$).

Fluorescence was measured on 2-mL samples in a thermostated cell at 25 °C with an Aminco-Bowman spectrophotofluorometer using an activation wavelength of 350 nm and emission wavelength of 380 nm. Because a narrow entrance slit width was used and only the initial time course of fluorescence intensity changes was analyzed, it was not necessary to correct the fluorescence measurements for bleaching. To convert fluorescence intensity to actin polymer concentration, a determination of the critical actin concentration was made prior to and under the ionic conditions of each experiment (Kouyama & Mihashi, 1981). Atomic absoption measurements were performed with a Model 103 Perkin-Elmer atomic absoption spectrophotometer. Radioactivity was measured with a Model 4530 Packard Tricarb liquid scintillation system.

Stock ^{45}Ca-labeled monomeric actin was prepared by overnight incubation of actin (10–20 μM concentration) with dialysis solution containing 0.02 mM $^{45}CaCl_2$ (specific activity 3.3–10.8 μCi/mol). The amount of tightly bound Ca^{2+} per mole of protein was determined by the polymerization and ultracentrifugation method described below. EGTA/Mg^{2+} treatment of ^{45}Ca-actin was performed by adding EGTA and $MgCl_2$ each to final concentrations of 0.05 mM and incubating for 6 min. Actin and its bound cation were separated from the $^{45}Ca^{2+}$ in the buffer by polymerization and ultracentrifugation, and by column separation.

Polymerization and Ultracentrifugation. Samples of ^{45}Ca-actin before and after EGTA/Mg^{2+} treatment were fully polymerized within 2 min by addition of KCl to 100 mM and equimolar (with actin) phalloidin (Estes et al., 1981). After centrifugation at 151000*g* for 3 h, the surfaces of the actin pellets were washed 3 times with 2 mL of 100 mM KCl and 2 mM Tris, pH 7.8, dissolved in 0.5 N NaOH, and then diluted to 0.06 N NaOH for radioactivity and atomic absorption measurements. Supernatant entrapped in the pellet was determined by using unlabeled actin samples to which ^{45}Ca was added *after* actin was polymerized by KCl/phalloidin addition. After centrifugation, the pellets were treated the same as experimental samples. Actin-bound Ca^{2+} and Mg^{2+} were calculated from measurements of $^{45}Ca^{2+}$ and Mg^{2+} in the pellets and supernatants, with correction for supernatant entrapped in the pellet.

Column Separation. ^{45}Ca-actin after EGTA/Mg^{2+} treatment was chromatographed on a column of Sephadex G-50 preequilibrated with a solution of 0.2 mM ATP, 0.05 mM EGTA, 0.05 mM $MgCl_2$, 2 mM Tris, pH 7.8, and 0.01% NaN_3. Elution of the protein peak required 2 min. Total Mg^{2+} in the protein peak and in the eluant was measured to determine bound Mg^{2+}. ^{45}Ca was measured in the column protein peak to estimate residual bound Ca^{2+}; this amount does not directly reflect the bound Ca^{2+} level at the end of the 6-min EGTA/Mg^{2+} treatment, which may be higher due to Ca^{2+} loss from the protein peak during passage through the column.

Results

The polymerization of N-P-labeled monomeric actin containing Ca^{2+} as the bound cation (Ca^{2+}-actin) is usually induced by the addition of either KCl, $MgCl_2$, or $CaCl_2$ at $t = 0$ as demonstrated in Figure 1A. Under each condition shown, polymerization begins with a lag phase, during which time the nucleation step is generally thought to occur. Given enough time, polymer formation can be detected at each salt concentration shown, even with 0.55 mM $CaCl_2$, which exhibits a very slow rate of polymerization. That this lag phase is primarily due to nucleation is demonstrated in Figure 1B, where polymerization was monitored under the same conditions as Figure 1A but after the addition of both salt and 50 μL of 2.5 μM phalloidin-stabilized actin nuclei (seeds) (see Experimental Procedures) at $t = 0$. Clearly, the linear curves indicate the lag phase is completely eliminated when KCl or $CaCl_2$ is added with seeds to stimulate polymerization. The slight initial upward curvature observed with added 1 mM $MgCl_2$ and seeds indicates that under this condition the lag phase is still present but considerably reduced.

If the polymerization of Ca^{2+}-actin is induced by low concentrations of $MgCl_2$, the presence of a lag phase is even more apparent. Figure 2A (curve C) illustrates the characteristic lag phase when polymerization is induced by the addition of only 0.3 mM $MgCl_2$ at $t = 0$. Strikingly, when both 0.3 mM $MgCl_2$ and 50 μL of 2.5 μM phalloidin-stabilized actin nuclei are added at $t = 0$ (curve B), the lag phase, although shorter, is still present. If the monomeric actin is preincubated for 7 min with 0.3 mM $MgCl_2$ before seeds are added at $t = 0$, then polymerization occurs without a lag phase, as shown by curve A. This could be explained by a Mg^{2+}-induced activation step in the polymerization of actin, or it could be due to the exchange of the actin-bound Ca^{2+} for Mg^{2+}, forming Mg^{2+}-actin.

To differentiate between these two possibilities, actin polymerization was monitored under the same conditions as used

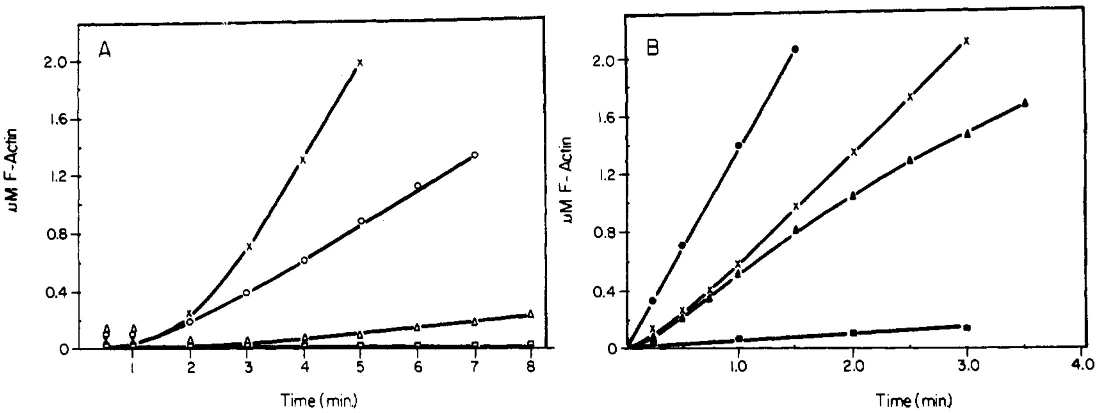

FIGURE 1: (A) Actin polymerization stimulated by the addition of neutral salt. Monomeric actin (7 μM) labeled with *N*-(1-pyrenyl)iodoacetamide was polymerized by the addition of (final concentrations) 100 mM KCl (○), 1 mM $MgCl_2$ (×), 1 mM $CaCl_2$ (△), or 0.55 mM $CaCl_2$ (□). Conditions: 0.2 mM ATP, 0.02 mM $CaCl_2$, 0.01% NaN_3, and 2 mM Tris, pH 7.8, 25 °C. (B) Actin polymerization stimulated by the addition of neutral salt and 50 μL of phalloidin-stabilized seeds. Conditions same as in (A). Actin polymerized with (all concentrations final) 100 mM KCl (●), 1 mM $MgCl_2$ (×), 1 mM $CaCl_2$ (▲), and 0.55 mM $CaCl_2$ (■), added at $t = 0$.

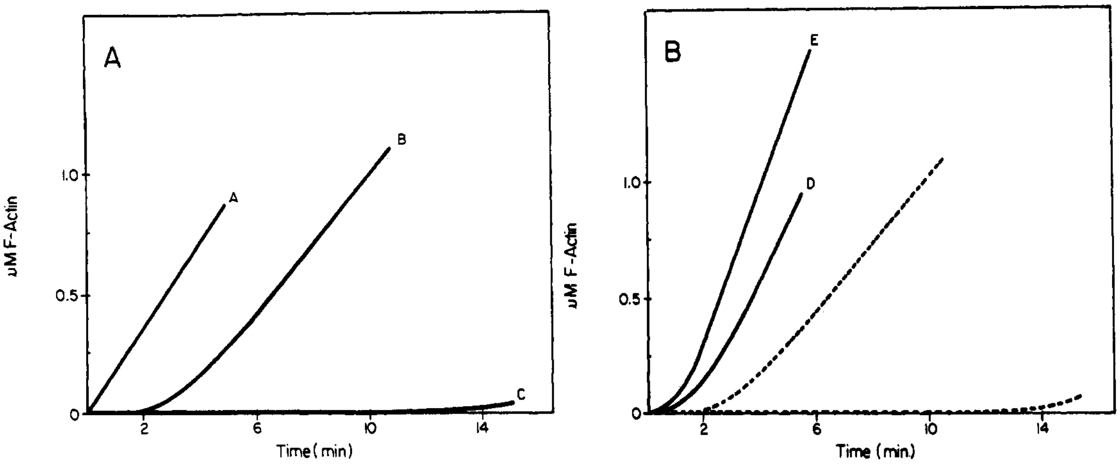

FIGURE 2: (A) Actin polymerization stimulated by the addition of 0.3 mM $MgCl_2$. Monomeric actin (7 μM) was polymerized by the addition of $MgCl_2$ only to a final concentration of 0.3 mM (curve C), 0.30 mM $MgCl_2$ and 50 μL of phalloidin-stabilized seeds at $t = 0$ (curve B), and 0.3 mM $MgCl_2$ added to the actin 7 min before the seeds were added at $t = 0$ (curve A). Other conditions same as in Figure 1A. (B) Actin polymerization stimulated by $MgCl_2$ addition in the presence of EGTA. Conditions same as in (A) except 0.025 mM EGTA (curve D) or 0.05 mM EGTA (curve E) was also added at $t = 0$ (solid lines). Dashed lines are curves B and C from Figure 2A.

in Figure 2A, but with EGTA also added at $t = 0$. The solid curves in Figure 2B show the polymerization of actin after addition at $t = 0$ of 0.3 mM $MgCl_2$, 50 μL of 2.5 μM phalloidin-stabilized seeds, and 0.025 mM EGTA (curve D) or 0.05 mM EGTA (curve E). The dashed lines are the same data as in Figure 2A and are included in Figure 2B for comparison. In the presence of EGTA, the lag phase, although still present, is shorter. This result is consistent with the facilitated removal of actin-bound Ca^{2+} by EGTA and its replacement by Mg^{2+}.

To directly demonstrate the replacement of actin-bound Ca^{2+} by Mg^{2+} after incubation of Ca^{2+}-actin with 0.05 mM EGTA and 0.05 mM $MgCl_2$, measurements of the actin-bound cation were made before and after treatment with EGTA and Mg^{2+}. The results (Table I) show that the initial Ca^{2+}-actin contained no detectable Mg^{2+} and 0.9 mol of Ca^{2+} bound/mol of actin. After incubation with EGTA/Mg^{2+} for 6 min, the radioactivity measurements showed less than 0.1 mol of Ca^{2+} bound/mol of actin, and estimation of the Mg^{2+} by atomic absorption showed 0.9–1.2 mol of Mg^{2+} bound/mol of actin. Both methods of separating actin from its incubation medium gave comparable results. Clearly, cation exchange occurs over an interval comparable to the nucleation-independent lag phase, producing Mg^{2+}-actin monomer.

Table I: Actin-Bound Divalent Cation before and after Incubation with EGTA and $MgCl_2$

	method of separation[a]	mol of cation/ mol of actin	
		Ca	Mg
initial ^{45}Ca-actin	A	0.9	0
EGTA/Mg^{2+} treated ^{45}Ca-actin	A	<0.1	1.2
	B	0.04	0.9

[a] Method A, polymerization and ultracentrifugation; method B, column separation. See Experimental Procedures for explanation of methods. Table entries are averages of four determinations.

Further studies were performed to characterize the formation of Mg^{2+}-actin from Ca^{2+}-actin. Monomer actin with bound Ca^{2+} was incubated with either 0.025 or 0.05 mM EGTA and either 0.05 or 0.3 mM $MgCl_2$. After various times of incubation, 50 μL of 2.5 μM phalloidin-stabilized seeds was added, plus enough $MgCl_2$ to make the final $MgCl_2$ concentration in every sample 0.3 mM, and the initial rate of polymerization of each sample was determined. Figure 3 shows a plot of the initial rate of polymerization vs. the time of incubation with EGTA. The rate of polymerization was greatest when actin was incubated with 0.3 mM $MgCl_2$ and either 0.05 or 0.025 mM EGTA or with 0.05 mM $MgCl_2$ and 0.05 mM EGTA. Under conditions of incubation where the EGTA concentration was not high enough (0.025 mM) to

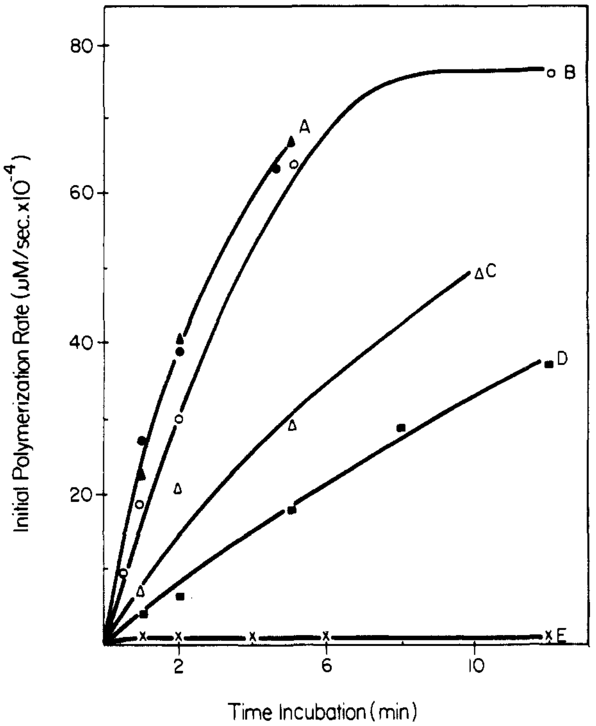

FIGURE 3: Initial polymerization rates of monomeric actin after incubation with EGTA and/or $MgCl_2$. Monomeric actin (7 μM) was incubated for various time intervals with EGTA and/or $MgCl_2$. At the end of the incubation period, polymerization was initiated by addition of 50 μL of 2.5 μM phalloidin-stabilized actin nuclei and $MgCl_2$ to 0.3 mM final concentration; thus, samples incubated at varying $MgCl_2$ concentrations (0, 0.05, and 0.3 mM) all had the same $MgCl_2$ concentration (0.3 mM) present at the time the polymerization rate was assayed. The initial polymerization rate was measured as the average over the first 30 s of the polymerization time course and is plotted (ordinate) against the time of incubation (abscissa). Conditions for sample incubation: solid symbols, incubated with 0.3 mM $MgCl_2$ and (●) 0.050 mM EGTA, (▲) 0.025 mM EGTA, or (■) 0 mM EGTA; open symbols, incubated with 0.05 mM $MgCl_2$ and (○) 0.050 mM EGTA or (△) 0.025 mM EGTA; (×) incubated with 0 mM $MgCl_2$ and 0.050 mM EGTA. All samples also contained 0.2 mM ATP, 0.02 mM $CaCl_2$, 2 mM Tris-HCl, pH 7.8, and 0.01% NaN_3.

completely chelate the bound Ca^{2+} and the free Mg^{2+} concentration was low (0.05 mM), the initial rate of polymerization was slower. As controls, an intermediate rate of polymerization was obtained with actin incubated with 0.3 mM $MgCl_2$ only in the absence of EGTA, and no *initial* polymerization could be detected when actin was incubated with 0.05 mM EGTA only. Clearly, the maximum polymerization rates were obtained under conditions where exchange of the actin-bound Ca^{2+} for exogenous Mg^{2+} would be expected to be optimal.

The data in Figure 3 indicate several interesting points regarding the formation of monomeric Mg^{2+}-actin: (1) As the EGTA concentration that actin is incubated with is increased, the rate of formation of Mg^{2+}-actin is also increased (compare curves B–D). (2) At least some Mg^{2+} must be present during the incubation period because, if Mg^{2+} is omitted, no initial rate of polymerization is detectable (curve E). (3) At low EGTA concentrations, the rate of formation of Mg^{2+}-actin is increased by higher $MgCl_2$ concentrations (compare solid circles and triangles with open circles and triangles). (4) Under the conditions studied, the maximum rate of formation of Mg^{2+}-actin shows a time constant on the order of 180 s, estimated from curve A. (5) Mg^{2+}-actin appears to polymerize rapidly since the highest initial rates of polymerization were obtained when conditions were optimal for its formation (Selden et al., 1983). Tobacman & Korn (1983) as well as Borejdo et al. (1983) have reported comparable properties for Mg^{2+}-actin.

Discussion

The results presented in this study clearly show that when the nucleation phase is circumvented, a lag phase is still observable when Ca^{2+}-actin is polymerized with moderate concentrations of $MgCl_2$. This nucleation-independent lag phase is not present when Ca^{2+}-actin is polymerized with KCl or $CaCl_2$ or when Mg^{2+}-actin is polymerized with $MgCl_2$, $CaCl_2$, or KCl (data not shown). That the duration of the lag phase when Ca^{2+}-actin is polymerized with $MgCl_2$ is affected by EGTA, or by preincubation with Mg^{2+}, strongly suggests that divalent cation exchange is a principal event occurring during this nucleation-independent lag phase. Measurements of the cation bound to actin verify that Mg^{2+} replaces Ca^{2+} as the bound divalent cation during this lag phase. The formation of monomeric Mg^{2+}-actin from Ca^{2+}-actin is associated with a time constant on the order of 180 s, which compares quite favorably with the 70–120 s calculated by Korn (1982) for the exchange of the actin-bound Ca^{2+} from the data of Kuehl & Gergely (1969). Differences between the time constant we obtained for Ca^{2+} release (and Mg^{2+} binding) and that reported for bound Ca^{2+} exchange could be due to differences in cation binding under our conditions. Subsequent conformational changes in monomeric actin after Mg^{2+} replaces the bound Ca^{2+} have been reported (Frieden et al., 1980; Frieden, 1982) but are likely to occur on a faster time scale. Thus, there appears to be exchange of the tightly bound divalent cation early during the course of polymerization of Ca^{2+}-actin in the presence of Mg^{2+}. Probably this divalent cation exchange accounts for what has been termed the monomer activation step (Pollard et al., 1982; Cooper et al., 1983; Gershman et al., 1983).

Acknowledgments

We thank Dr. Carl Moos for helpful discussions of portions of this work. We also acknowledge the excellent typing assistance of Mary Peplowski, Maureen Davis, Deborah Moran, and Marie Stoddard.

Registry No. Ca, 7440-70-2; Mg, 7439-95-4.

References

Borejdo, J., Garty, N., Shimon, T., Oplatka, A., & Muhlrad, A. (1983) in *Actin: Structure and Function in Muscle and Non-Muscle Cells* (dos Remedios, C. G., & Barden, J., Eds.) pp 123–128, Academic Press, Australia.

Bradford, M. (1976) *Anal. Biochem. 72*, 248–254.

Brenner, S. L., Tobacman, L. S., & Korn, E. D. (1983) in *Actin: Structure and Function in Muscle and Non-Muscle Cells* (dos Remedios, C. G., & Barden, J., Eds.) pp 97–106, Academic Press, Australia.

Cooper, J. A., Buhle, E. L., Walker, S. D, Tsong, T. Y., & Pollard, T. D. (1983) *Biochemistry 22*, 2193–2202.

Estes, J. E., Selden, L. A., & Gershman, L. C. (1981) *Biochemistry 20*, 708–712.

Frieden, C. (1982) *J. Biol. Chem. 257*, 2882–2886.

Frieden, C., Lieberman, D., & Gilbert, H. (1980) *J. Biol. Chem. 255*, 8991–8993.

Gershman, L. C., Selden, L. A., Estes, J. E., & Newman, J. (1983) *Biophys. J. 41*, 95a.

Gilbert, H., & Frieden, C. (1983) *Biochem. Biophys. Res. Commun. 111*, 404–408.

Kasai, M., Asakura, S., & Oosawa, F. (1962) *Biochim. Biophys. Acta 57*, 22–31.

Biochemistry **1984**, *23*, 2203–2210

Korn, E. D. (1982) *Physiol. Rev. 62*, 672–737.

Kouyama, T., & Mihashi, K. (1981) *Eur. J. Biochem. 114*, 33–38.

Kuehl, W. M., & Gergely, J. (1969) *J. Biol. Chem. 244*, 4720–4729.

Oosawa, F., & Asakura, S. (1975) *Thermodynamics of the Polymerization of Protein*, Academic Press, New York.

Pollard, T. D., Aebi, V., Cooper, J. A., Fowler, W. E., Kiehart, D. P., Smith, P. R., & Tseng, P. C. (1982) *Philos. Trans. R. Soc. London, Ser. B 299*, 237–245.

Selden, L. A., Estes, J. E., & Gershman, L. C. (1983) *Biochem. Biophys. Res. Commun. 116*, 478–485.

Szent-Gyorgyi, A. (1951) *Chemistry of Muscular Contraction*, 2nd ed., Academic Press, New York.

Tobacman, L. S., & Korn, E. D. (1983) *J. Biol. Chem. 258*, 3207–3214.

Mass Transport and Reaction Kinetic Parameters Determined Electrochemically for Immobilized Glucose Oxidase[†]

James F. Castner[‡] and Lemuel B. Wingard, Jr.*

ABSTRACT: Mass-transfer resistances often have pronounced effects on the overall reaction rates of enzymes immobilized at interfaces or in polymeric matrices. In the present work glucose oxidase was immobilized on the surface of a platinum disk electrode by one of three attachment techniques: silane–glutaraldehyde, allylamine–glutaraldehyde, and albumin–glutaraldehyde. In one group of studies the electrodes were rotated, and methods were employed to determine the diffusion and shielding coefficients for transport of a model electroactive compound, i.e., potassium ferrocyanide, through the enzyme matrix. A model electrochemically active compound was used because glucose exhibits a very slow rate of electron transfer at a platinum surface. The diffusion coefficient for ferrocyanide was reduced 7% by the silane–enzyme and 25% by the allylamine–enzyme matrices. In a second group of studies the electrodes were held stationary. Marked internal diffusional resistance was noted for the albumin–glutaraldehyde–enzyme matrix. The calculated flux of ferrocyanide was decreased by a factor of 2000–8500 for transport through albumin–enzyme matrices 0.21–0.063 cm thick, as compared to transport through free solution. In a third group of studies the rotating enzyme-matrix electrode was utilized in determining apparent values of the Michaelis constant for glucose. The velocity of the reaction was determined by amperometric measurement of the concentration of hydrogen peroxide reaching the ring electrode. The results, determined from Eadie–Hofstee type plots of reaction current and substrate concentration, gave values between 12 and 36 mM for the three methods of immobilization. The results show that the mass-transfer resistance for diffusion of small molecules through immobilized glucose oxidase varied with the method of enzyme coupling. This study also shows that electrochemical techniques are useful in defining the relative rates of mass transfer and enzymatic reaction.

Many of the enzymatic reactions that take place in cells and tissues occur at interfaces or within some type of membrane, rather than in homogeneous solution (McLaren & Packer, 1970). In such heterogeneous sytems the kinetics of enzyme-catalyzed reactions may be quite different than in homogeneous solution (Engasser & Horvath, 1974). In particular, the rates at which substrates or products diffuse through the enzyme matrix may become slower than the rate of the enzyme-catalyzed reaction. This diffusional resistance is an important consideration in the study and application of enzymes immobilized on artificial matrices or supports (Kasche, 1983). Diffusional resistances can arise from transport limitations at the interface between the bulk solution and the enzyme support (i.e., external resistance) or from transport limitations within the support matrix (i.e., internal resistance) (Engasser & Horvath, 1976). One of the perplexing problems in the study of enzyme-catalyzed reactions in heterogeneous systems is the experimental determination of the degree of diffusional resistance. Highly sensitive methods are required for measuring the rate of transport of material through the enzyme-support matrix without causing undue perturbation of the system.

Several electrochemical methods, based on rotating and stationary electrodes, fulfill the requirements for high sensitivity and lack of a need to take samples. Rotating ring disk electrodes (RRDE)[1] are especially well suited for characterizing the rates of transport of material through an enzyme-support matrix (Bard & Faulkner, 1980); yet this technique has received surprisingly little application to date. A typical RRDE is shown in Figure 1. The disk and ring are insulated from each other and connected by lead wires to external circuitry. With suitable auxiliary and reference electrodes, the potential or current at the disk or ring can be controlled or measured. An enzyme matrix can be attached to the disk, and the RRDE can be rotated while immersed in a solution of substrate or other diffusate. When the RRDE is operated at different rotation speeds, the external diffusional resistance for the substrate can be selectively controlled, thus enabling the measurement of internal diffusional limitations. For characterization of external or internal mass-transfer resistances, the diffusate must undergo very rapid oxidation or reduction at the electrode in order not to influence the results of the measurements.

The RRDE was used to study the mass-transfer/reaction kinetics of glucose oxidase attached via octadecylamine, glutaraldehyde, and albumin to a carbon paste disk (Shu &

[†] From the Department of Pharmacology, School of Medicine, University of Pittsburgh, Pittsburgh, Pennsylvania 15261. *Received August 29, 1983.* This work was supported by Grant R01 AM26370 from the National Institutes of Health.

[‡] Present address: Photoproducts Department, E. I. du Pont de Nemours & Co., Wilmington, DE 19898.

[1] Abbreviation: RRDE, rotating ring disk electrode.

0006-2960/84/0423-2203$01.50/0